LE THUY HANG, M.Sc.,N.A.
Technical University of Gdańsk
Faculty of Ocean Engineering
and Ship Technology

Calculation of the influence of propeller operation on the hydrodynamic characteristics of the rudder

SUMMARY

The paper presents a lifting surface method for calculation of the hydrodynamic characteristics of the rudder in the propeller slipstream. Flow velocity induced by the propeller in given points on the rudder is calculated. Pressure distribution, lift and drag of the rudder is computed with taking into account propeller interaction. The calculation results show good consistence with experimental data.

INTRODUCTION

In most cases the classical rudders, i.e vertical hydrofoils of symmetrical profile sections located at a short distance behind ship propeller, are influenced by an unsteady propeller slipstream. The propeller accelerates and rotates the inflow into the rudder. The hydrodynamic performance of the propeller and rudder is determined by the flow field around them. It differs from the case when each of them is working alone. This is the most visible consequence of the propeller – rudder interaction.

This paper presents a calculation method based on the lifting surface theory. For a rudder of known geometry, located within a known, non-uniform velocity field the method supplies the following information :

- the velocity field induced by the propeller on the rudder
- pressure distribution on the rudder with and without propeller interaction
- rudder lift and drag with propeller interaction at different propeller advance coefficients.

The paper presents description of the method as well as example calculation results compared with the experimental data.

CALCULATION OF THE PROPELLER - - INDUCED VELOCITY FIELD

The presented method makes it possible to calculate the velocity field induced by a propeller of arbitrary geometry, operating in the surrounding space, in particular on the rudder located in the propeller slipstream. The propeller may operate in uniform or non - uniform inflow velocity field, thus local differences in propeller blade loading can be taken into account. The induced velocity is calculated in a given set of points located on the rudder.

The computational model of the propeller blade presented in Fig.1 is similar to that described in [2] and [7]. The lifting surface is built of the mean lines of respective blade sections and bounded by the blade outline. A number of bound vortex elements is located in several chordwise strips defined on the lifting surface. Each discrete, bound vortex element represents in fact vorticity distributed continuously over the elementary blade area. In order to fulfil the Kelvin theorem on vorticity conservation the elements must be supplemented with the system of trailing vortex elements. The intensity of the trailing vortex elements can be expressed by a combination of the intensities of the bound vortex elements in the adjacent strips of the lifting surface. After leaving the blade trailing edge the trailing vortices form the free vortex system extending, in theory, up to infinity. Free vortex lines are not acted upon by forces and they should follow the local streamlines. Consequently, their geometry should be established by calculating the velocity field behind the propeller including the effect of the free vortices themselves. This would require a complicated and time consuming iterative process. The studies and analyses performed by other authors [3] demonstrated that the influence of limited variations in the geometry of the free vortices caused only meaningless differences in the calculated velocity field. Therefore it was decided to assume that the pitch of the free vortex surfaces can be predicted a priori by using the following formula :

$$\varphi_w = a\,\varphi_B + (1-a)\beta \qquad (1)$$

where :

φ_w - pitch angle of the free vortex line
φ_B - pitch angle of the blade section
a - experimentally correlated coefficient;
  a = 0.8 was applied in the presented calculations
β - inflow angle at the radius in question.

Moreover, the contraction of the propeller slipstream is neglected without compromising the results. Thus the geometry of the entire vortex system is considered as known, and only the intensities of all vortex elements must be calculated.

Furthermore, it is assumed that the unsteady effects resulting from propeller operation in the non-uniform velocity field behind the ship hull are of secondary importance for the propeller–rudder interaction. They are appropriately represented by a quasi-steady approach in which varying intensity of the free vortices is not required. The length of the free vortex surfaces behind the propeller can be also limited to 5 revolutions of the helix without reducing the accuracy of the induced velocities calculated either on the propeller or on the rudder. If the free vortex lines hit the rudder in any particular position of the propeller they terminate on the rudder surface.
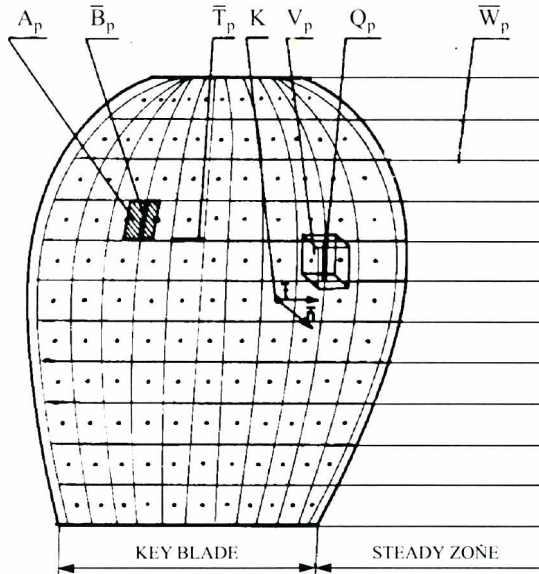

Fig.1. Discrete vortex/source model of the propeller blade

The thickness of the blades is represented by discrete sources (or sinks) located in the same points as the bound vortex elements. A linearized approach is adopted in which the system of vortices and sources may be treated independently, i.e. without their mutual interaction. Consequently, the intensity of sources may be a priori calculated by using the following formula :

$$q = \left| \overline{V} + \overline{\omega}R \right| \frac{dt}{dx} \Delta R \qquad (2)$$

where :

q	-	source (sink) intensity
$\overline{V}$	-	inflow velocity
$\overline{\omega}$	-	angular velocity of propeller rotation
R	-	radius at which a given point of calculation is located
$\dfrac{dt}{dx}$	-	derivative of blade thickness in the direction of inflow
ΔR	-	radial extent of a chordwise strip.

Now the intensities of the bound vortex elements remain the only unknown quantity in the lifting surface model. These intensities can be calculated by using the kinematic boundary condition together with the Kutta condition at the blade trailing edge. The kinematic boundary condition on the lifting surface requires that the resultant relative velocity of flow at the surface should be tangent to this surface. This condition is the basis for the following integral equation :

$$\frac{1}{4\pi} \left[\iint_{S_p} \overline{n} \gamma_B \nabla \left(-\frac{1}{r} \right) dS + \iint_{S_w} \overline{n} \gamma_w \nabla \left(-\frac{1}{r} \right) dS \right] =$$

$$= -\iint_{S_p} q \frac{\partial}{\partial n} \left(-\frac{1}{r} \right) dS - \left(\overline{V} + \overline{\omega}R \right) \overline{n} = 0 \qquad (3)$$

where :

$\overline{n}$	-	unit length vector normal to the lifting surface
γ_B	-	vorticity distribution over the blades
γ_w	-	vorticity distribution over the free vortex surfaces
q	-	source distribution modelling the blade thickness
r	-	distance between the blade area element and the point of calculation
S_p	-	area of the blades
S_w	-	area of the free vortex surfaces.

In the discrete model the above defined kinematic boundary condition is tested in a number of control points located on the lifting surface (Fig.1). It has been proved that if these points are located in the middle of the quadrangles formed by the adjacent vortex elements, the discrete formulation is fully equivalent to the continuous one given by (3). In the discrete formulation the following equation can be written for every control point (all velocities represent local normal components on the lifting surface) :

$$\sum_{i=1}^{M} H_{ij} \Gamma_i = -V_{Qj} - \sqrt{V_j^2 + \left(2\pi R_j m \right)^2} \qquad (4)$$

where :

H_{ij}	-	influence coefficient relating j-th control point to i-th vortex element
Γ_i	-	intensity of i-th vortex element
V_{Qj}	-	velocity induced at j-th point by all sources modelling blade thickness
V_j	-	inflow velocity at j-th point
R_j	-	radius at which j-th point is located
m	-	number of propeller revolutions per second.

Analogous equations applied to all control points form the system of linear equations comprising the unknown intensities of the bound vortex elements. This system includes equations corresponding to all control points on all propeller blades i.e. it represents the entire propeller. In this situation there are more unknowns than equations – one excessive unknown in each chordwise strip. This problem is cured by means of the Kutta condition : *the bound vorticity modelling the tangential velocity difference between the sides of the lifting surface, should be zero at the trailing edge.*

The right hand side of the system includes the normal components of the known velocities, i.e. velocities induced by sources and the external inflow velocities. The latter can be interpolated from the non-uniform velocity field at the propeller plane if only such field is known. Solution of that system of linear equations leads to the value of Γ.

Once the intensities of all bound vortex elements on the lifting surfaces are known, the velocity induced by the propeller in an arbitrary point in the surrounding space (in particular on the rudder) can be easily calculated (Fig.2).
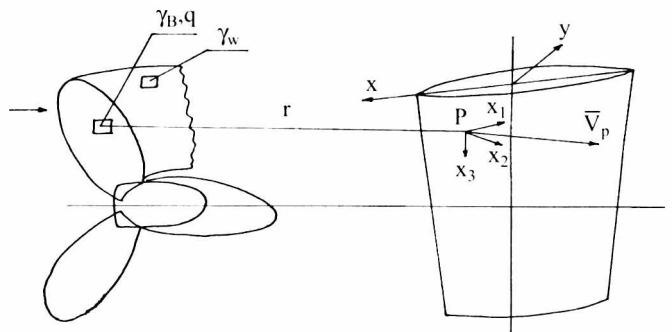

Fig.2. Calculation of the velocity induced by the propeller on the rudder

In the computation point P an arbitrarily oriented orthogonal system of three unit length vectors $\{x_1, x_2, x_3\}$ is defined and the propeller-induced velocity is described by three components defined in the system. The propeller-induced velocity $\overline{V}_p$ is calculated for a number of equally spaced angular positions of the propeller, then an

arithmetic average is taken to calculate the mean value of the velocity in the respective point. The Biot-Savart formula is used again for the vortex-induced velocity, together with the appropriate formula for the source-induced velocity.

Different grid densities of the discrete representation of the propeller were numerically tested and it was concluded that in the typical propeller – rudder configuration the acceptable accuracy can be achieved by relatively sparse system of vortices and sources. In this system 25 bound vortex elements are assumed on each blade (5 strips with 5 elements each), i.e. for instance, a five-blade propeller can be described by 100 linear equations. The remaining 25 elements are determined by the Kutta condition applied at the trailing edge of the blades. In the result of further numerical tests it was decided that performing the calculations for 5 angular positions of the propeller is sufficient to produce satisfactorily accurate mean velocities induced at the rudder.

CALCULATION OF THE HYDRODYNAMIC CHARACTERISTICS OF THE RUDDER

The lifting surface theory applied to the rudder model is based on the discrete distribution of vortex elements modelling the hydrodynamic loading as well as on the discrete distribution of sources and sinks modelling the rudder thickness. This approach is similar to that applied for the propeller.

The rudder surface is divided into a discrete system of concentrated vortex and source elements instead of the continuous distribution of the vortices and sources, as shown in Fig.3. In the vertical direction, eight sections are used to divide the rudder into chordwise strips. Along each strip, eleven bound vortex elements B_p are located in the Z - axis direction. The vorticity continuously distributed over the elementary area A_p is replaced by the bound vortex element B_p. According to Kelvin theorem on conservation of circulation, each chordwise strip is separated from its neighbour by a series of the trailing vortex elements T_p. It should be noted that all intensities of the trailing vortex elements can be expressed in terms of the bound vortex element intensities. Moreover, the bound vortex elements always point towards the rudder tip and the trailing vortex elements always point towards the trailing edge. If the grid is sufficiently dense, the bound and trailing vortex elements can reflect accurately the hydrodynamic load distribution over the rudder.

Locations of the control points K used to satisfy boundary condition are chosen in the middle of the rectangles formed by the vectors $\bar{B}_p$ and $\bar{T}_p$. The locations of the points are defined by the radii $R_{K(i)}$ (i = 1, 2, 3,....) and the coordinate along the chord, $x_{K(j)}$. (j = 1, 2, 3,....). In practical calculations, the control points are located at : 0.0425, 0.0925, 0.1525, 0.2225, 0.3025, 0.3925, 0.4925, 0.6025, 0.7225, 0.8525 of the chord length from the leading edge of each strip. In other words, the control points are considered as the central point of the straight line joining the midpoints of the two nearest bound or trailing vortex elements.

The number of control points is equal to the number of independent bound vortex elements. It should be noted that the Kutta condition is applied, i.e. at the trailing edge the bound vorticity is equal to zero, so the number of unknown intensities of bound vortex elements is decreased by one in each chordwise strip.

At all control points the unit vectors normal to the surface are calculated by taking the vector product of two vectors tangent to the lifting surface $\bar{B}_p$ and $\bar{T}_p$.

Except the vortex lines, a grid of sources and sinks is distributed on the rudder to simulate its finite thickness. The discrete sources coincide with the location of bound vortex elements characterizing the blade circulation. These sources form straight-line segments of continuous and uniform distribution of strength. They are co-linear with the vectors $\bar{B}_p$ but are not vectors themselves.

It is assumed that the effect of the rudder thickness does not affect significantly the pressure distribution on the rudder. Therefore the intensities of the sources and sinks Q_p are calculated only once for every analysed rudder geometry and then used for all given angles of attack.

Due to the Kelvin theorem on vorticity conservation, a system of free vortices is formed behind the rudder. In theory this system should extend downstream to infinity, but in practice it is sufficient to terminate it somewhere. It is considered that free vortices are located on a plane surface extending from the rudder trailing edge and inclined at an angle β to the X - Z plane. On the basis of an extensive correlation analysis, β is taken equal to 0.5 of the angle-of-attack α. The vorticity distribution in the free vortex system contributes to the induced velocity at the control points. (Fig.3)
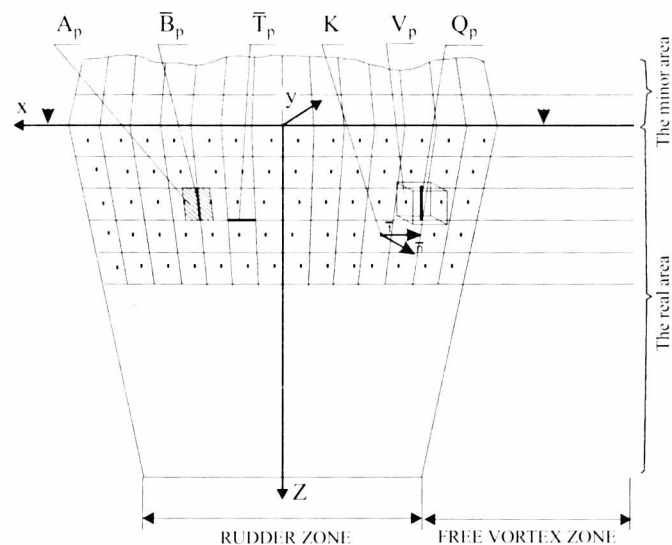
Fig.3. *Discrete vortex/source model of the rudder blade*

Formulation of this method is based on the kinematic boundary condition. It states that at every point on the rudder the vector component of the velocity flow normal to that surface should be equal to zero. The boundary condition is mathematically defined as follows :

$$\sum V_{\Gamma N} + \sum V_{QN} + \sum V_N = 0 \qquad (5)$$

or

$$\sum V_N = 0 \qquad (6)$$

where :

$V_{\Gamma N}$ - normal velocity induced by the vorticity distribution on the lifting surface including free vortices

V_{QN} - normal component of the velocity induced by the sources distribution simulating the rudder thickness

V_N - normal component of the inflow velocity.

In the rudder model there are two kinds of singularities inducing velocities in the control point : line vortex segments and sources or sinks.

To determine velocities induced by the vortex lines in the control point, the law of Biot – Savart is used in the following form :

$$\overline{V}_C = \frac{k\Gamma}{4\Pi} \frac{\bar{r}\bar{l}}{r^3} \qquad (7)$$

where :

Γ - circulation intensity of the element

$\bar{r}$ - distance vector

$\bar{l}$ - element vector

$\overline{V}_C$ - induced velocity vector, normal to the plane defined by $(\bar{r}, \bar{l})$ resulting from the analytical integration along l

k - correction coefficient.

If r is much larger than l, the above given formula is sufficiently accurate. In this case k = 1 is used. If r is less than 5 x l, the following formula for the correction coefficient is used :

$$k = \left[\frac{r\cos\delta + \frac{1}{2}l}{\sqrt{(r\sin\delta)^2 + (r\cos\delta + \frac{1}{2}l)^2}} - \right.$$

$$\left. + \frac{r\cos\delta - \frac{1}{2}l}{\sqrt{(r\sin\delta)^2 + (r\cos\delta - \frac{1}{2}l)^2}} \right] \frac{r}{l\sin^2\delta} \qquad (8)$$

where :

δ - angle contained between $\bar{r}$ and $\bar{l}$.

The formula (8) is developed on the basis of exact integration of the velocity induced by the vortex element *l* in the point located close to the element.

The second kind of singularity on the rudder are the sources simulating the finite thickness of the rudder. The velocity induced by an element source in the control point can be calculated by using the following formula :

$$\overline{V}_Q = \frac{q}{4\Pi}\frac{\bar{r}}{r^3} \qquad (9)$$

where :

V_Q - source induced velocity in the direction consistent with *r*
q - source (sink) intensity
$\bar{r}$ - length of the vector connecting the source with the control point.

Moreover, a mirror image of the rudder with the respect to the free surface is introduced in order to take into account the free surface influence on the hydrodynamic characteristics. Velocities induced in the control points by the free vortex elements and the mirror image are calculated similarly to the calculation of the induced velocities of trailing and bound vortex lines on the rudder.

Now the system of linear equations for unknown intensities B_p reflecting the boundary condition on the rudder, is set up. As mentioned previously, the boundary condition requires that no flow normal to the lifting surface is permitted. Each equation of the system refers to the particular control point on the rudder lifting surface and it has the following form :

$$\sum_{i=1}^{M} H_{Ni}G_i = -V_N - V_{QN} \qquad (10)$$

where :

H_{Ni} - line of the induced factor matrix H_N referring to the control point in question
G_i - unknown intensities of the bound vortex elements in the discrete lifting surface of the rudder
V_N - normal component of the inflow velocity at the control point in question, including the propeller induced velocity
V_{QN} - normal component of the velocity induced at the control point in question by the system of sources simulating the blade thickness.

In the above defined system there is one unknown more than the number of equations in each chordwise strip. The Kutta condition is again employed to solve this situation as it requires that the bound vorticity between the sides of the lifting surface should be zero at the trailing edge.

The coefficients H_{Ni} are calculated on the basis of the Biot – Savart formula. The right hand side of the system includes the normal component of the known velocities.

After solving this system, the intensities of vortices forming the lifting surface are determined. Now the velocities induced by the vortex system of the rudder may be calculated explicitly. The intensities of sources simulating the rudder thickness are already known. The velocities induced by them are given in the exact form. They are projected onto the directions tangent and normal to the rudder surface, to

be used in evaluation of the boundary condition and in calculation of the rudder pressure distribution. The resultant flow velocity on the rudder may be calculated.

On the basis of the resultant velocity of flow on both pressure and suction side, the pressure distribution on the rudder, given in the form of the non-dimensional pressure coefficient C_p, is evaluated using Bernoulli equation.

$$C_p = 1 - \frac{V_G^2}{V_i^2} = \frac{p - p_0}{\frac{1}{2}\rho V_i^2} \qquad (11)$$

where :

V_G - resultant velocity at the point in question (vector sum of the inflow and the induced velocity – different for the suction and for the pressure side of the rudder)
V_i - inflow velocity at the point in question
p - pressure at the control point in question
p_0 - pressure at infinity
ρ - density of water.

The pressure distribution calculated by means of the formula (11) corresponds to potential flow and it must be corrected for the effect of viscosity. The viscosity correction factor μ_1 developed in [9] is aplied to C_p.

$$\mu_1 = (1 + 0.87T)\left[1 - e^{(-0.0691 + 12.46\,T - 0.1855\ln Re)}\right] \qquad (12)$$

where :

T - maximum relative thickness of the section profiles
Re - Reynolds number.

Apart from the viscosity correction the pressure distribution is also corrected for the effect of the leading edge radius. The correction factor μ_2 is determined according to the formula developed by Lighthill [8]. It removes the infinite pressure value at the leading edge, which appears normally in the lifting surface calculation.

$$\mu_2 = \frac{x_K}{x_K + \frac{1}{2}d_{LE}} \qquad (13)$$

where :

x_K - chordwise coordinate of the control point
d_{LE} - radius of the leading edge of the rudder section.

· Finally, the pressure distribution used in calculation of the hydrodynamic forces and moments on the rudder can be written as :

$$C_p^* = C_p\mu_1\mu_2 \qquad (14)$$

When the pressure distribution over the blade is calculated, the evaluation of resulting force and moment components generated on the rudder is performed.

An element of the rudder area is assigned to each control point. It is assumed that the pressure distribution over this element is uniform and equal to C_p^* calculated for the control point. The calculation of the elementary lift and drag is performed in the following way :

$$L = (C_{pP}^* - C_{pS}^*)\frac{1}{2}\rho V_\infty^2 A_p \qquad (15)$$

$$D = C_D\frac{1}{2}\rho V_\infty^2 A_p \qquad (16)$$

where :

C_{pP}^* - pressure coefficient on the pressure side
C_{pS}^* - pressure coefficient on the suction side
C_D - drag coefficient
A_p - area of the element.

The elementary lift L and drag D can be resolved into three force components : F_x, F_y, F_z and three moment components : M_x, M_y, M_z. It should be noticed that the rudder section has large thickness, so it should be taken into account in calculation of L and D by applying the additional leading edge suction force. The values of the six components for the whole rudder are obtained by integrating over the rudder area.

RESULTS
OF EXAMPLE CALCULATIONS

The experimental investigation of A.F. Molland and S.R. Turnock [1] was selected to perform the example calculation of the propeller – rudder interaction.

The all – movable rudder used in the calculation has a rectangular plane form with 667 mm chord, NACA 0020 section and 1000 mm span. The propeller is of four blades, 800 mm diameter and 0.4 blade area ratio. In Tab.1 the geometrical particulars of the propeller are given.

Tab.1. Geometrical particulars of the propeller (modified Wageningen B4.40 Series)

Number of blades	4
Range of revolutions [rpm]	0 to 3000
Diameter [mm]	800
Boss diameter (max) [mm]	200
Mean pitch ratio	0.95 (set for tests)
Blade area ratio	0.40
Rake [deg]	0
Blade thickness ratio t/D	0.050
Section form	Based on Wageningen B series
Blade outline form	Based on Wageningen B but with reduced skew

Rudder force and moment was computed for values of the rudder incidence angle α contained within the range of $-40°$ to $+40°$, generally at each of 5° increments, with and without propeller influence. The rudder incidence angle α is defined with respect to the propeller axis (Fig.4). Moreover the drift angle β, defined between the undisturbed inflow direction and propeller axis, is taken into account.
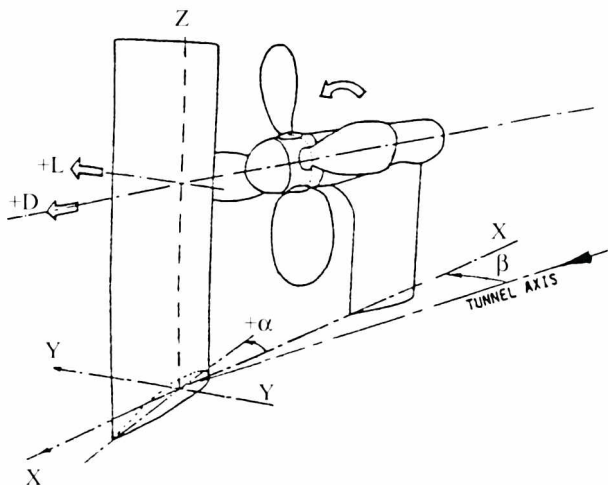

Fig.4. Schematic view of the propeller – rudder arrangement

The calculations were made for the constant flow speed of 10 m/s and different values of the propeller advance ratio (J = 0.51, 0.36 and 0.94). The drift angle $\beta = 7.5°$ is used in the presentation. The calculation results include the following fields :

Velocity field induced by the propeller on the rudder

The flow velocity induced by the propeller in given points on the rudder can be calculated for each of the five angular positions of the propeller. The final result is the arithmetic average of the five values. The component velocity field is defined by x_1, x_2, x_3 in the rectangular coordinate system OXYZ (Fig.2). Normal and tangential components of the propeller induced velocity on the rudder are shown in Fig.5 and 6. The quantities are plotted as functions of $\overline{x}_c$ and $\overline{z}_b$ over the $\overline{X}$ - $\overline{Z}$ plane in the figure as coordinate of control points had been developed to the $\overline{X}$ - $\overline{Z}$ plane.

$$\overline{x}_c = \frac{x}{c} \quad \text{and} \quad \overline{z}_b = \frac{z}{b}$$

where:
- b – span of the rudder
- c – chord of the rudder
- x, z – longitudinal and vertical coordinate in the Cartesian OXYZ
- $\overline{x}_c$ – non-dimensional coordinate along the chord
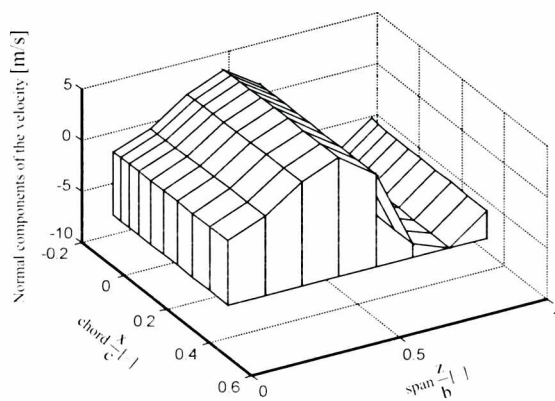- $\overline{z}_b$ – non-dimensional coordinate along the span

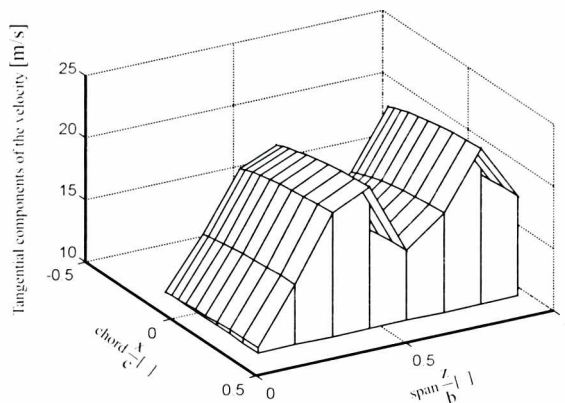*Fig.5. Normal components of the velocity on the rudder; included propeller influence, $\alpha = 5°$, $\beta = 0°$*

Fig.6. Tangential components of the velocity on the rudder; included propeller influence, $\alpha = 5°$, $\beta = 0°$

Pressure distribution on the rudder with and without propeller influence

The calculated pressure distributions on both suction (C_{pS}) and pressure side (C_{pP}) of the rudder at some selected rudder incidence angles, with and without accounting for propeller influence are presented in Fig.7, 8, 9 and 10. The figures show the degree of influence of propeller operation on the pressure distribution on the rudder. For example, in the case of : $\alpha = 5°$, $\beta = 0°$ and J = 0.51 (Fig.7) the pressure on both sides of the isolated rudder is investigated. When the propeller influence is included (Fig.8) the pressure becomes markedly different on both sides of the rudder. The effect of propeller influence is different in the areas above and below the propeller axis. There is no doubt that the hydrodynamic performance of rudder located behind an operating propeller is markedly different from that of an isolated rudder of the same geometry.
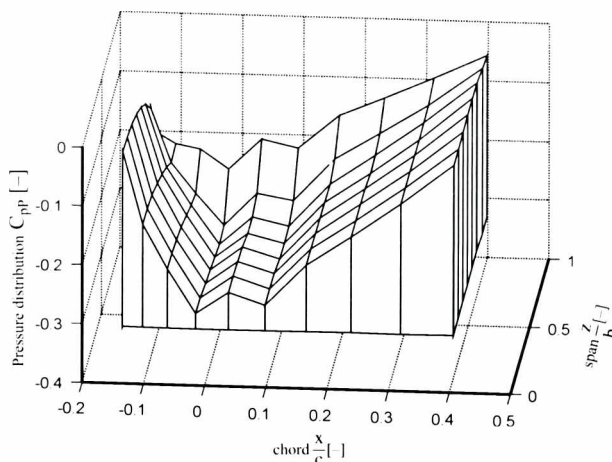

Fig.7. Distribution of the pressure coefficient C_{pP}; not included propeller influence, $\alpha = 5°$, $\beta = 0°$
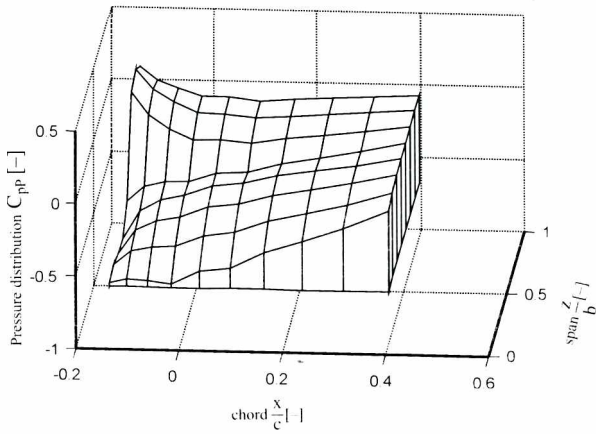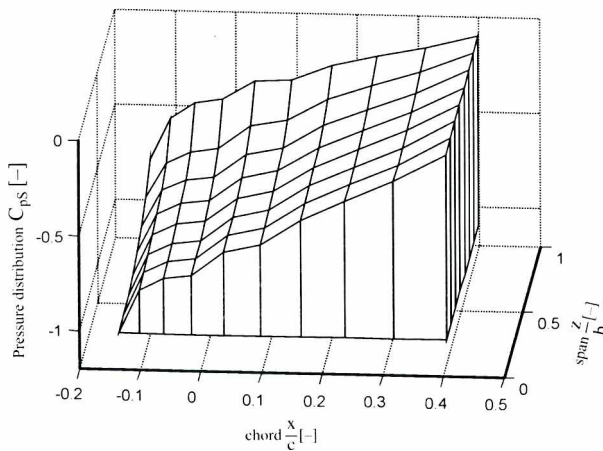
Fig.8. *Distribution of the pressure coefficient C_{pP} ; included propeller influence, $\alpha = 5°$, $\beta = 0°$*

Fig.9. *Distribution of the pressure coefficient C_{pS} ; not included propeller influence, $\alpha = 5°$, $\beta = 0°$*
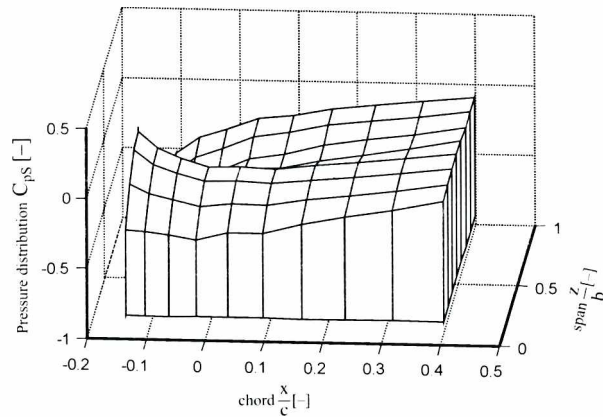

Fig.10. *Distribution of the pressure coefficient C_{pS} ; included propeller influence, $\alpha = 5°$, $\beta = 0°$*

Lift and drag of the rudder including propeller influence at different propeller advance ratios

Results of the calculations are presented in Fig.12 and Fig.14 in the form of rudder hydrodynamic characteristics (the lift coefficient C_L and drag coefficient C_D) in function of the rudder incidence angle α, for three values of the propeller advance ratio J. In general, they agree well with experimental results shown in Fig.11 and 13. The results demonstrate how strongly the forces on the rudder depend on the loading and performance of the propeller.
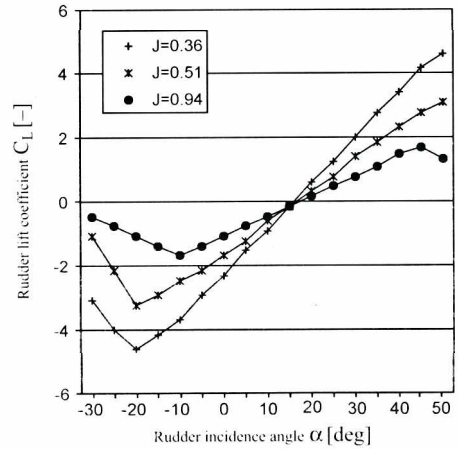

Fig.11. *Effect of the propeller advance ratio J on the performance of the rudder at the drift angle $\beta = 7.5°$ (experiment)*
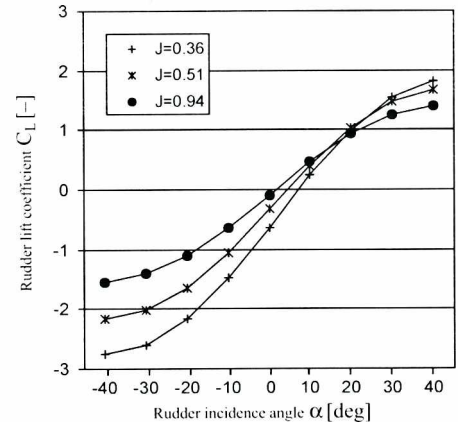

Fig.12. *Effect of the propeller advance ratio J on the performance of the rudder at the drift angle $\beta = 7.5°$ (calculation)*

Fig.13. *Effect of the propeller advance ratio J on the performance of the rudder at the drift angle $\beta = 7.5°$ (experiment)*

Fig.14. *Effect of the propeller advance ratio J on the performance of the rudder at the drift angle $\beta = 7.5°$ (calculation)*
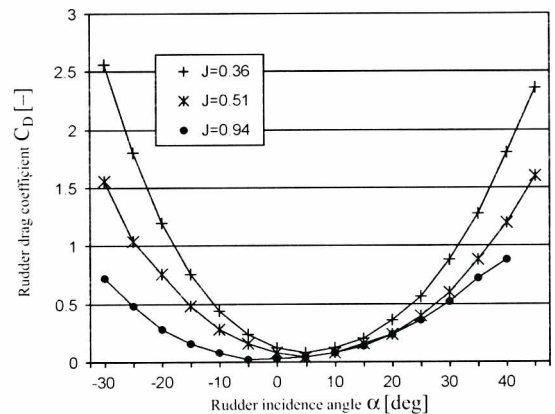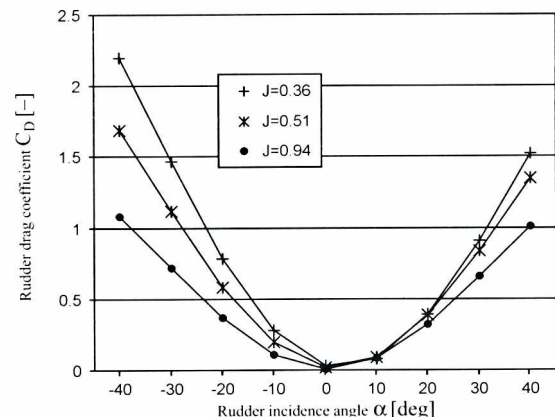
CONCLUSIONS

◆ The lifting surface method described in this paper makes it possible to obtain information on operation of the rudder in non--uniform inflow velocity field with propeller interaction, namely : velocity field in slipstream, pressure distribution on the rudder, force and moment components, influence of propeller loading on the rudder performance.

◆ In order to determine influence of the propeller on the rudder, the actual velocity distribution in the propeller slipstream on the rudder is calculated. The obtained characteristics of the rudder confirm that the lift force (lift coefficient C_L) is a function of many parameters of which the operating conditions of the propeller and position of the rudder in the propeller slipstream are the most important.

◆ The calculation results demonstrate the importance of the effective drift angle on the performance of the rudder – propeller system. They appear accurate for various practical applications. This method may be applied in rudder design as well as in evaluation of ship manoeuvring ability to increase ship safety and effectiveness.

In this paper only the propeller – rudder interaction was studied. In fact, the ship hull has also an influence on the system. Therefore future development of the method presented in this paper is focused on accounting for the effect of hull – propeller – rudder interaction.

Appraised by Jan Szantyr, Prof.,D.Sc.,N.A.

NOMENCLATURE

A_p - elementary area
B_p - bound vortex element
C_D - rudder drag coefficient
C_L - rudder lift coefficient
C_p - pressure coefficient
C_{pP} - pressure coefficient on the pressure side
C_{pS} - pressure coefficient on the suction side
D - drag force
H - influence coefficient
K - control point
l - element vector
L - lift force
m - number of propeller revolutions per second
n - unit length vector normal to the lifting surface
p - pressure at the control point in question
p_o - pressure at infinity
q - the source (sink) intensity
Q_p - source element
r - distance between the blade area element and the point of calculation
R - radius at which point of calculation is located
t - unit lenght tangential vector at the lifting surface
T_p - trailing vortex element
V - inflow velocity
V_C - induced velocity
V_G - resultant velocity at the point in question (vector sum of the inflow and the induced velocity – different for the suction and for the pressure side of the rudder)
V_p - volume element
V_Q - velocity induced by the sources distribution simulating the rudder / propeller thickness
V_T - tangential component of the inflow velocity
V_Γ - normal velocity induced by the vorticity distribution
W_p - free vortex element
$\overline{X}$ - non-dimensional coordinate along the chord
$\overline{Z}$ - non-dimensional coordinate along the span
α - rudder incidence angle
β - drift angle
Γ - the intensity of the circulation of the element
δ - angle between vortex element and distance vector
γ_B - vorticity distribution on the lifting surface
γ_W - vorticity distribution on the free vortex surfaces
μ_1 - viscosity correction factor
μ_2 - leading edge radius correction factor
ρ - density of water
ω - angular velocity of propeller rotation

Indices:

i - index of the vortex element   N - normal component
j - index of the control point   * - value corrected for effect of viscosity
K - control point   — - vector

BIBLIOGRAPHY

1. Molland A.F. and Turnock S.R.: *The Effect of the Hull on the Manoeuvring Performance of Rudders*. Proc. International Conference on Ship Motion & Manoeuvrability. RINA. London, 1998
2. Glover E.J., Szantyr J.A.: *The Unsteady Lifting Surface Program for Analysis of the Propeller Response to the Non-uniform Inflow Field*. University of Newcastle Upon Tyne, Emerson Cavitation Tunnel. Report No.6/83
3. John P.Breslin, Poul Andersen: *Hydrodynamics of Ship Propellers*. Cambridge University Press. 1994
4. Krishnamurty Karamcheti: *Principles of Ideal – Fluid Aerodynamics*. John Wiley & Sons, Inc. 1966
5. Le Thuy Hang: *A Lifting Surface Method for Calculation of Hydrodynamic Forces on the Rudder*. Marine Technology Transactions, 1999, Vol.10,
6. Shiu – Wu Chau: *Computation of Rudder Force and Moment in Uniform Flow*. Ship Technology Research, 1998, Vol.45, No.1
7. Szantyr J.A.: *A Method for Analysis of Cavitating Marine Propeller in Non-uniform Flow*. International Shipbuilding Progress, 1994, Vol.41, No.427
8. Thwaites B.: *Incompressible Aerodynamics*. Oxford University Press. 1960
9. W.F.Bavin et al.: *Ship Propellers – Contemporary Calculation Methods* (in Russian). Ed. Sudostroenie. Leningrad 1983.

*C*onference

METNET
Seminar and Workshop
in Gdynia

Within the scope of 5th Program of European Union, the Gdynia Maritime Academy actively takes part in realization of five , out of fourteen , tasks provided in the project of European Commission's Thematic Network on Maritime Education, Training and Mobility of Seafarers (METNET).

It concerns one of the main problems of the worldwide maritime economy (important especially for the EU countries), i.e. considerable shortage of ship officers of the qualifications complying with the standards of STCW'95 International Convention adopted by about 140 countries. In the Convention great emphasis is placed on safety at sea and protection of marine environment worldwide.

Accelerated technological development, and especially application of computer techniques, brings new challenges and demands improved quality of solutions applied to maritime economy.

The World Maritime University in Malmö (Sweden), affiliated to International Maritime Organization (IMO), co-ordinates the project.

On 6 and 7 May this year a METNET seminar and scientific workshop was held, co-organized by Gdynia Maritime Academy, for the Central and East European countries and a group of selected West European countries, members of the consortium for realization of the METNET project.

The conference was chaired by Prof. Günther Zade, the project's co-ordinator and Vice-rector of the World Maritime University.

Representatives of maritime universities, scientific research centres as well as national maritime administrations from 14 countries, namely : Belgium, Bulgaria, Croatia, Estonia, Spain, Lithuania, Latvia, Germany, Romania, Slovenia, Sweden, Great Britain, Hungary and Poland, took part in the events.

The subject matter of the seminar and workshop was focused on the Maritime Education and Training (MET), especially on :

◆ number of students resulting from predictions on future employment in the worldwide maritime economy
◆ shaping scientific development and qualifications of the didactic personnel of the maritime universities
◆ syllabuses and
◆ financing of MET.